

UC Irvine

UC Irvine Previously Published Works

Title

Formulation of two-photon and two-gluon decays of pseudoscalar η mesons in a relativistic bound-state calculation

Permalink

<https://escholarship.org/uc/item/7q57z7m2>

Journal

Physical Review D, 36(11)

ISSN

2470-0010

Authors

Silverman, Dennis
Yao, Heng

Publication Date

1987-12-01

DOI

10.1103/physrevd.36.3392

Copyright Information

This work is made available under the terms of a Creative Commons Attribution License, available at <https://creativecommons.org/licenses/by/4.0/>

Peer reviewed

Formulation of two-photon and two-gluon decays of pseudoscalar η mesons in a relativistic bound-state calculation

Dennis Silverman and Herng Yao

Department of Physics, University of California, Irvine, California 92717

(Received 22 June 1987)

We formulate a relativistic bound-state calculation of the decay of η (0^{-+}) mesons into two gluons or two photons. The decays of η_c , η'_c , η_b , and η'_b are calculated and a value of α_s deduced from the total width of η_c . The calculated value for $\eta_c \rightarrow 2\gamma$ is in agreement with experiment. The decays of $\eta \rightarrow 2\gamma$ and $\eta' \rightarrow 2\gamma$ are calculated and by comparison with experiment and the bound on $\iota \rightarrow 2\gamma$, restrictions are placed on the X_η , Y_η , $X_{\eta'}$, and $Y_{\eta'}$ mixing coefficients of Rosner. The comparison with the Schrödinger-equation calculations shows that the inclusion of relativistic propagators spreads out the annihilations so that they do not occur at $r=0$. This suppresses the $2S$ and higher-level decays, with the greatest suppression for the lightest quarks.

I. INTRODUCTION

In order to evaluate the relativistic corrections to bound-state mesonic spectra in QCD, and to establish the relativistic nature of the parts of the QCD potential, a relativistic expansion of the quark field equation was formulated^{1,2} using a valence-quark-antiquark pair in the lowest order for the meson states. This type of equation has a long history,³ including successful QED calculations of positronium.⁴ In this paper we extend this relativistic formalism to the two-gluon and two-photon annihilations of the 0^{-} meson states. We then apply this and compare with data for the $\eta_c \rightarrow 2$ gluon rate and predict the $\eta_b \rightarrow 2$ gluon rate. In this we find that the value of α_s that fits the two-gluon rate is $\alpha_s \simeq 0.15$. We also calculate the decay $\eta_c \rightarrow \gamma\gamma$ and find this in agreement with experiment. We finally apply the decay formalism to η and $\eta' \rightarrow 2$ photon states and illustrate how the differences in the wave functions between $s\bar{s}$ and $(u\bar{u} + d\bar{d})$ components as well as higher-order QCD corrections can be important in the comparison with experiment. With a parameter for higher-order QCD corrections and the bound on $\iota \rightarrow 2\gamma$ we find the restrictions that our calculations place on the X_η , Y_η , $X_{\eta'}$, and $Y_{\eta'}$ mixing parameters of Rosner in a standard mixing models to account for the η , η' , and ι mixing. We compare the relativistic rates to those obtained from the Schrödinger equation using the nonrelativistic limit of the relativistic interactions.

We also compare the η decay rates computed with an asymptotic-freedom-corrected gluon exchange with those computed from a vector Coulomb interaction⁵ (both with a linear scalar part) in order to determine if the results are sensitive to the asymptotic-freedom modification of single-gluon exchange.

In the relativistic valence-quark bound-state equation we used a relativistic vector-gluon exchange corrected by an asymptotically free coupling strength, along with a linear confining potential which was established to have a scalar nature.^{1,2} The resulting equation, after partial-wave projection, is a single-variable integral equation for

the radial wave functions in momentum space with the mass of the state as the eigenvalue. It reduces to the Breit-Fermi interaction in the Schrödinger-equation limit, and to the Dirac equation in the limit where one quark mass is much heavier than the other. In the first papers,^{1,2} the studies were concerned mainly with the spectra, emphasizing the relativistic spin-spin and spin-orbit effects. The spectra and wave functions were calculated for all mesons except the chiral-symmetry-dominated π and K mesons.

The relativistic nature is most important in short-distance or high-momentum phenomena and in cases involving light-mass quarks where the Schrödinger equation is a poor approximation since the momenta are typically larger than the light-quark (u , d , or s) constituent masses. In this paper we treat both types of cases, calculating them with relativistic amplitudes and using relativistic wave functions obtained from the previous fits to the spectra.

In Sec. II we summarize the relativistic wave functions and bound-state equation that was previously formulated and used in calculations of the mesonic spectra.^{1,2} In Sec. III we formulate relativistically the decay of η mesons into two gluons and two photons in terms of the relativistic η wave functions. In Sec. IV we apply this to the η_c , η'_c , η_b , and η'_b decay to two gluons and two photons. In Sec. V we examine the η and η' decays to two photons and illustrate the wave-function effects in a simple standard model which includes mixtures of η_8 and η_1 with a glueball⁶ to form the η , η' , and ι states. Using the bounds on $\iota \rightarrow 2\gamma$ and a parameter for higher-order QCD corrections, we show the restrictions placed on the mixing parameters of this model.

II. FORMULATION OF THE RELATIVISTIC BOUND-STATE EQUATION

The equation we use is based on the equation for the quark field $\psi(x)$ with mass m_1 , coupled to a vector gauge potential $A_\mu(x)$, and an effective scalar potential $S(x)$:

$$(i\nabla - m_1)\psi(x) = [\mathbf{A}(x) + S(x)]\psi(x). \quad (2.1)$$

The bound-state equation is obtained from the matrix element of Eq. (2.1) between the bound state of four-momentum B and an antiquark state of mass m , momentum p , and spin λ :

$$(i\nabla - m_1)\langle \mathbf{p}, \lambda | \psi(x) | B \rangle = \sum_n \langle \mathbf{p}, \lambda | \mathbf{A}(x) + S(x) | n \rangle \langle n | \psi(x) | B \rangle, \quad (2.2)$$

where a complete set of states has been inserted. The lowest-mass state is the single on-shell antiquark state which we will use and consider it as the valence-quark approximation. This then leads to a linear integral equation for the matrix elements $\langle \mathbf{p}, \lambda | \psi_\alpha(0) | B \rangle$. With energies $\omega_B = (\mathbf{B}^2 + M^2)^{1/2}$, $\omega = (\mathbf{p}^2 + m^2)^{1/2}$, and with M the bound-state mass we define the 4×4 matrix

$$\Phi_{\alpha\beta}(B, p) = (2\pi)^3 \left[\frac{2\omega_B \omega}{m} \right]^{1/2} \sum_\lambda \langle \mathbf{p}, \lambda | \psi_\alpha(0) | B \rangle \bar{v}_\beta(p, \lambda). \quad (2.3)$$

We introduce the analogs of Dirac equation components in 2×2 submatrices

$$\Phi = \begin{bmatrix} \tilde{G}_u & \tilde{G}_d \\ \tilde{F}_u & \tilde{F}_d \end{bmatrix}, \quad (2.4)$$

where u and d stand for upper and lower \bar{q} components

$$\begin{aligned} G_d(\mathbf{p}) &= g_0(p) | J=0, M_J=0; L=0, S=0 \rangle \langle J=0, M_J=0; L=0, S=0 |, \\ F_d(\mathbf{p}) &= f_+(p) | J=0, M_J=0; L=1, S=1 \rangle \langle J=0, M_J=0; L=1, S=1 |. \end{aligned} \quad (2.8)$$

Working out the projection operator gives (dropping an inessential overall i factor)

$$\begin{aligned} G_d &= \frac{g_0}{\sqrt{8\pi}} \sigma_y \quad \text{or} \quad \tilde{G}_d = \frac{g_0}{\sqrt{8\pi}}, \\ F_d &= -\frac{f_+}{\sqrt{8\pi}} \sigma \cdot \hat{\mathbf{p}} \sigma_y \quad \text{or} \quad \tilde{F}_d = -\frac{f_+}{\sqrt{8\pi}} \sigma \cdot \hat{\mathbf{p}}. \end{aligned} \quad (2.9)$$

For the details of the bound-state equation for $g_0(p)$ and $f_+(p)$ we refer the reader in Refs. 1 and 2. We are using a modified form of the cutoff with a variable power $\epsilon > 0$ representing the effect of inelastic channels:

$$S_\epsilon(\Lambda_0, p) = \left[\frac{\Lambda_\epsilon^2}{\Lambda_\epsilon^2 + \mathbf{p}^2} \right]^{1+\epsilon} \quad (2.10)$$

with $\Lambda_\epsilon = \Lambda_0 \sqrt{1+\epsilon}$. Expanding this for small \mathbf{p}^2/Λ_0^2 shows that the cutoff in the predominant region of \mathbf{p}^2 is independent of ϵ .

We can most conveniently take traces using a pseudoscalar form for Φ defined in terms of Dirac matrices that also satisfies the on-shell antiquark condition, Eq. (2.5). The form has two invariant functions $a(p), b(p)$:

and G and F stand for upper and lower quark components. We note the restrictions arising from Eq. (2.3) that

$$\Phi(p)(\not{p} + m) = 0 \quad (2.5)$$

which means that \tilde{G}_u, \tilde{F}_u can be taken as dependent on \tilde{G}_d, \tilde{F}_d by

$$\tilde{G}_u = -\tilde{G}_d \frac{\sigma \cdot \mathbf{p}}{\omega + m}, \quad \tilde{F}_u = -\tilde{F}_d \frac{\sigma \cdot \mathbf{p}}{\omega + m}. \quad (2.6)$$

In order to do the spin and angular momentum decomposition we convert the $\bar{2}$ representation for the antiquarks to a 2 representation by defining $G_d = \tilde{G}_d \sigma_y$ and $F_d = \tilde{F}_d \sigma_y$ so we can use conventional Clebsch-Gordan coupling. We then have

$$\langle \mathbf{p}, \lambda | \psi(0) | B \rangle = \frac{i(-1)^{\lambda-1/2}}{(2\pi)^3} \frac{2m}{[2\omega_B \omega(\omega+m)]^{1/2}} \begin{bmatrix} G_d \\ F_d \end{bmatrix} \chi_\lambda. \quad (2.7)$$

In the integral equations the matrix Φ occurs naturally, and we will use it in much of the formulation.

For the wave-function decomposition we expand $G_d(\mathbf{p})$ and $F_d(\mathbf{p})$ in terms of $Y_L^{M_L}(\hat{\mathbf{p}})$ and 2×2 projection operators for $S=0$ and $S=1$ states, coupling them to the total J and M_J . The η states, $J^P=0^-$, are unnatural-parity states and since $J=0$ they only involve two instead of the four wave functions used^{1,2} when $J \neq 0$. In the general formalism this becomes

$$\Phi = \gamma_5 \left[a(p) + b(p) \frac{\not{B}}{M} \right] \frac{\not{p} - m}{2m}. \quad (2.11)$$

Reducing this to the form of Eq. (2.4) yields

$$\tilde{G}_d = \left[\frac{\omega - m}{2m} \right] (-a + b), \quad \tilde{F}_d = -(a + b) \frac{\sigma \cdot \mathbf{p}}{2m}. \quad (2.12)$$

Comparison with Eq. (2.9) then gives $a(p), b(p)$ in terms of the solutions to the bound-state integral equation $f_+(p), g_0(p)$:

$$\begin{aligned} a &= \frac{1}{4\sqrt{2\pi}} \frac{2m}{\omega + m} \left[-g_0 + \frac{\omega + m}{p} f_+ \right], \\ b &= \frac{1}{4\sqrt{2\pi}} \frac{2m}{\omega + m} \left[g_0 + \frac{\omega + m}{p} f_+ \right]. \end{aligned} \quad (2.13)$$

The normalization condition becomes

$$\frac{1}{M} \int \frac{d^3 p}{(2\pi)^3} \left[a^2 + b^2 - 2 \frac{m}{\omega} ab \right] = 1. \quad (2.14)$$

III. DECAY OF AN η MESON INTO TWO GLUONS OR TWO PHOTONS

We formulate the decay of a $0^- q\bar{q}$ meson (η) with quark masses $m_1=m_2=m$ into two gluons or two photons using a relativistic amplitude and the valence-quark approximation. We begin with two photons and later add the color factors for the gluons. For an η of momentum B decaying into photons of momenta $q_1 \equiv q$ and q_2 we have, by reduction,⁷

$$\langle q_1 \lambda_1, q_2 \lambda_2 | B \rangle = \frac{1}{(2\pi)^3 (4q_1^0 q_2^0)^{1/2}} \epsilon^{\mu*}(q_1 \lambda_1) \epsilon^{\nu*}(q_2 \lambda_2) \times \int d^4 x_1 \int d^4 x_2 e^{iq_1 \cdot x_1} e^{iq_2 \cdot x_2} \langle 0 | T(J_\mu(x_1) J_\nu(x_2)) | B \rangle \quad (3.1)$$

with $J_\mu(x) = eQ\bar{\psi}(x)\gamma_\mu\psi(x)$. At this stage we have effectively used two orders of the $J^\mu A_\mu$ Hamiltonian to create the final-state photons or gluons, and in the valence-quark approximation can now treat the ψ fields in J_μ as in fields.

We want to evaluate the matrix element with a field annihilating the quark in the meson state on the right, so we use Wick's theorem to convert the time-ordered product to normal-order products, and using the fact that the η state is a superposition of $b^\dagger d^\dagger | 0 \rangle$ leads to two nonzero terms:

$$\langle 0 | T(J_\mu(x_1) J_\nu(x_2)) | B \rangle = \langle 0 | T(\psi(x_1)_\alpha [\bar{\psi}(x_2)\gamma_\nu]_\beta) | 0 \rangle \langle 0 | :[\bar{\psi}(x_1)\gamma_\mu]_\alpha \psi(x_2)_\beta : | B \rangle + \langle 0 | T(\psi(x_2)_\beta [\bar{\psi}(x_1)\gamma_\mu]_\alpha) | 0 \rangle \langle 0 | :[\bar{\psi}(x_2)\gamma_\nu]_\beta \psi(x_1)_\alpha : | B \rangle . \quad (3.2)$$

In the matrix elements of the normal-ordered terms only the product of the db or positive-frequency parts contributes, and we evaluate these by inserting a complete set of antiquark states between them and restoring the negative-frequency parts of the fields (which give zero) in the matrix elements:

$$\begin{aligned} \langle 0 | :[\bar{\psi}(x_2)_\beta \psi(x_1)_\alpha] : | B \rangle &= \sum_s \int d^3 p \langle 0 | \bar{\psi}(x_2)_\beta | \mathbf{p}s \rangle \langle \mathbf{p}s | \psi(x_1)_\alpha | B \rangle \\ &= \int d^3 p e^{i[p \cdot (x_1 - x_2) - B \cdot x_1]} \left[\frac{m}{(2\pi)^3 \omega} \right]^{1/2} \sum_s \langle \mathbf{p}s | \psi(0)_\alpha | B \rangle \bar{v}_\beta(\mathbf{p}s) \\ &= \frac{1}{[(2\pi)^3 2\omega_B]^{1/2}} \int \frac{d^3 p}{(2\pi)^3} \frac{m}{\omega} e^{i[p \cdot (x_1 - x_2) - B \cdot x_1]} \Phi(B, p)_{\alpha\beta} . \end{aligned} \quad (3.3)$$

Replacing the vacuum matrix elements in Eq. (3.2) by propagators and converting to momentum space yields the amplitude with terms corresponding to direct and exchanged final-state photons (see Fig. 1):

$$\langle q_1 \lambda_1, q_2 \lambda_2 | B \rangle = \frac{e^2 Q^2 (2\pi)^4 \delta^4(B - q_1 - q_2)}{(2\pi)^{9/2} (8q_1^0 q_2^0 \omega_B)^{1/2}} \frac{m}{(2\pi)^3} \epsilon^{\mu*}(q_1 \lambda_1) \epsilon^{\nu*}(q_2 \lambda_2) T_{\mu\nu}(B, q) , \quad (3.4)$$

$$T_{\mu\nu} = \int \frac{d^3 p}{\omega} \left[\text{Tr} \left[\gamma_\nu \frac{B - \not{p} - \not{q} - m}{(B - p - q)^2 - m^2} \gamma_\mu \Phi(B, p) \right] + \text{Tr} \left[\gamma_\mu \frac{\not{q} - \not{p} + m}{(q - p)^2 - m^2} \gamma_\nu \Phi(B, p) \right] \right] . \quad (3.5)$$

We work in the center-of-mass frame with $\cos\theta = \hat{\mathbf{p}} \cdot \hat{\mathbf{q}}$ and use the on-shell conditions $q^2=0$, $(B-q)^2=0$, and $p^2=m^2$. The propagators become

$$\begin{aligned} (B - p - q)^2 - m^2 &= -M(\omega + p \cos\theta) , \\ (q - p)^2 - m^2 &= -q(\omega - p \cos\theta) . \end{aligned} \quad (3.6)$$

The amplitude contains integrals over the radial wave functions in $\Phi(B, p)$, $a(p)$, and $b(p)$, Eq. (2.13), which are

$$\begin{aligned} I_d &= \frac{1}{m} \int \frac{d^3 p}{2\omega} \frac{b(p)}{(B - p - q)^2 - m^2} , \\ I_e &= \frac{1}{m} \int \frac{d^3 p}{2\omega} \frac{b(p)}{-2p \cdot q} , \end{aligned}$$

and by Lorentz invariance

$$\frac{1}{m} \int \frac{d^3 p}{2\omega} \frac{a(p)p^\alpha}{(B - p - q)^2 - m^2} = H_B B^\alpha + H_q q^\alpha , \quad (3.7)$$

$$\frac{1}{m} \int \frac{d^3 p}{2\omega} \frac{a(p)p^\alpha}{-2p \cdot q} = J_B B^\alpha + J_q q^\alpha .$$

Multiplying by q_α or B_α we can find H_B , etc. Taking the traces leads to the combination

$$C' = I_d + I_e - H_B - H_q - J_B \quad (3.8)$$

and the result

$$T_{\mu\nu} = 4i \epsilon_{\alpha\beta\mu\nu} B^\alpha q^\beta C' \quad (3.9)$$

which is seen to be current conserving in $q_1=q$ and $q_2=B-q$. Evaluating the integrals in C' using Eq. (3.6) and defining $C = M^{3/2} m C' / [2(2\pi)^3]$ gives

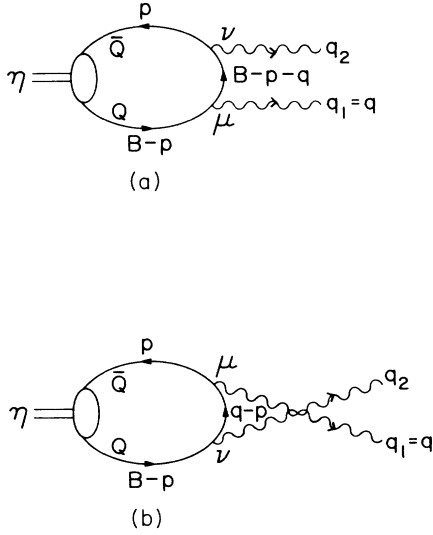


FIG. 1. Bound-state decay to two gluons or photons via valence-quark annihilation.

$$C = \frac{4\pi}{M^{1/2}} \int_0^\infty \frac{dp}{(2\pi)^3} \frac{p^2}{2\omega} \left[a(p) - b(p) \frac{m}{2p} \ln \left[\frac{\omega+p}{\omega-p} \right] \right]. \quad (3.10)$$

Including a color factor of 3 and denoting the Q^2 weighting in a superposition state as $\langle Q^2 \rangle$ we find the decay rate of an η -type meson to two photons to be

$$\Gamma_{\eta \rightarrow \gamma\gamma} = 48\pi\alpha^2 \langle Q^2 \rangle^2 C^2. \quad (3.11)$$

In the nonrelativistic⁸ limit $C \rightarrow \psi(0)/M$.

For η decay to two gluons the color factor is $\frac{2}{3}$ instead of 3, and with α_s the QCD coupling strength, we have

$$\Gamma_{\eta \rightarrow gg} = \frac{32\pi}{3} \alpha_s^2 C^2. \quad (3.12)$$

IV. HADRONIC AND RADIATIVE DECAYS OF η_c , η'_c , η_b , AND η'_b

A. Comparison of the calculated and experimental rates of $\eta_c \rightarrow 2g$ and $\eta_c \rightarrow 2\gamma$

Using the formula for the decay rate of η mesons to 2 gluons and 2 photons, Eqs. (3.11) and (3.12), we now calculate the rate for $\eta_c \rightarrow 2$ gluons. The rate is undetermined because of the α_s coupling to the “free” gluons, so we can use the experimental rate to give information on α_s at the η_c mass. Our calculated decay rates for $\eta_c \rightarrow 2g$ before the higher-order QCD corrections are

$$\Gamma_0(\eta_c \rightarrow 2g) = \left[\frac{\alpha_s}{0.185} \right]^2 11.5 \text{ MeV} \quad \text{for the } \epsilon = 1.0 \text{ cutoff,} \quad (4.1)$$

$$\Gamma_0(\eta_c \rightarrow 2g) = \left[\frac{\alpha_s}{0.185} \right]^2 12.7 \text{ MeV} \quad \text{for the } \epsilon = 0.25 \text{ cutoff.}$$

Comparison with the experimental value⁹ of the total η_c width

$$\Gamma(\eta_c) = 11.5 \pm 4.3 \text{ MeV} \quad (4.2)$$

shows this is consistent with $\alpha_s = 0.185$ to lowest order. It is also seen that the result is mostly independent of ϵ .

The wave functions give

$$C = 0.10 \text{ GeV}^{1/2} \quad \text{at } \epsilon = 1.0, \quad (4.3)$$

$$C = 0.11 \text{ GeV}^{1/2} \quad \text{at } \epsilon = 0.25.$$

The first-order QCD radiative correction to 0^{-+} to 2 gluons is given by Barbieri *et al.*¹⁰ as

$$\Gamma(0^{-+} \rightarrow 2g) = \left[1 + 10.6 \frac{\alpha_s}{\pi} \right] \Gamma_0(0^{-+} \rightarrow 2g). \quad (4.4)$$

Fitting this to the experimental value for the total η_c width, Eq. (4.2), determines a range of α_s for the $\eta_c \rightarrow 2g$ process

$$\alpha_s(\eta_c) = 0.15^{+0.02}_{-0.03} \quad \text{for } \epsilon = 1.0. \quad (4.5)$$

For this value of α_s , the first-order correction is 50% of the zeroth order, and higher orders may be important. From this $\alpha_s(\eta_c)$ we can find $\alpha_s(\eta_b)$, in order to predict the η_b width, by applying the running-coupling-constant formula which includes two-loop effects:¹¹

$$\alpha_s = \frac{4\pi}{\beta_0 \ln(x)} \left[1 - \frac{\beta_1 \ln[\ln(x)]}{\beta_0^2 \ln(x)} \right], \quad (4.6)$$

where $\beta_0 = 11 - \frac{2}{3}n_f$, $\beta_1 = 102 - \frac{38}{3}n_f$, and $x = Q^2/\Lambda_{\overline{\text{MS}}}^2$, where $\overline{\text{MS}}$ stands for the modified minimal-subtraction scheme. For η_c we use three flavors and for η_b four flavors, and assume that the effective Q 's scale up with the quark masses. For $\alpha_s(\eta_c)$ in Eq. (4.5) we have $\ln x(\eta_c) = 7.2^{+1.9}_{-1.1}$ and taking

$$\ln x(\eta_b) = \ln x(\eta_c) + 2 \ln(m_b/m_c) \quad (4.7)$$

we get $\ln x(\eta_b) = 9.5^{+1.9}_{-1.1}$. For these values we get

$$\alpha_s(\eta_b) = 0.13^{+0.01}_{-0.02}. \quad (4.8)$$

For charmonium, if we take $Q = 3 \text{ GeV}$ the limits in Eq. (4.5) are consistent with $\Lambda_{\overline{\text{MS}}}$ between 30 MeV and 140 MeV centered about 80 MeV and therefore not inconsistent with other determinations.

We now compare our calculated $\Gamma(\eta_c \rightarrow 2\gamma)$ with the experimental data.^{12,13} Our calculated decay rate for $\eta_c \rightarrow 2\gamma$ before the QCD correction is, for an $\epsilon = 1.0$ cutoff,

$$\Gamma_0(\eta_c \rightarrow 2\gamma) = 15.6 \text{ keV}. \quad (4.9)$$

The QCD-corrected decay rate¹⁴ is given by

$$\Gamma(\eta_c \rightarrow 2\gamma) = \left[1 - 3.38 \frac{\alpha_s}{\pi} \right] \Gamma_0(\eta_c \rightarrow 2\gamma). \quad (4.10)$$

Using $\alpha_s = 0.15^{+0.02}_{-0.03}$, which gives a 16% decrease for a QCD correction, we get

$$\Gamma(\eta_c \rightarrow 2\gamma) = 13.1 \pm 0.4 \text{ keV} . \quad (4.11)$$

The $\gamma\gamma \rightarrow \eta_c$ measurement gives¹²

$$\Gamma(\eta_c \rightarrow \gamma\gamma) = 15.0 \pm 6.3 \text{ keV} \quad (4.12)$$

while the $p\bar{p} \rightarrow \eta_c \rightarrow 2\gamma$ gives¹³

$$\Gamma(\eta_c \rightarrow \gamma\gamma) = 5.7_{-4}^{+5} \text{ keV} . \quad (4.13)$$

The weighted average¹²

$$\Gamma(\eta_c \rightarrow \gamma\gamma) = 9.2 \pm 3.9 \text{ keV} \quad (4.14)$$

is in agreement with our calculation, Eq. (4.11).

B. Predictions for η'_c , η_b , and η'_b decays to two gluons and two photons

Using $\alpha_s(\eta'_c) \simeq \alpha_s(\eta_c) = 0.15$ we can predict $\eta'_c \rightarrow 2g$ and 2γ from Eqs. (3.11) and (3.12) and QCD corrections Eqs. (4.4) and (4.10). These values are listed in Table I for the $\epsilon = 1.0$ and $\epsilon = 0.25$ cases. We give the values for the $\epsilon = 1.0$ cutoff only, where Γ_0 is without QCD corrections and Γ has QCD corrections:

$$\begin{aligned} C_{\eta'_c} &= 0.050 \text{ GeV}^{1/2} , \\ \Gamma_0(\eta'_c \rightarrow 2g) &= \left[\frac{\alpha_s}{0.15} \right]^2 1.82 \text{ MeV} , \\ \Gamma(\eta'_c \rightarrow 2g) &= \left[\frac{\alpha_s}{0.15} \right]^2 2.74 \text{ MeV} , \quad (4.15) \\ \Gamma_0(\eta'_c \rightarrow 2\gamma) &= 3.83 \text{ keV} , \\ \Gamma(\eta'_c \rightarrow 2\gamma) &= 3.21 \text{ keV} . \end{aligned}$$

Similarly, for η_b and $\eta'_b \rightarrow 2g$ and 2γ , we have the

values for the $\epsilon = 1.0$ case and for $\alpha(\eta_b) = 0.13$:

$$\begin{aligned} C_{\eta_b} &= 0.075 \text{ GeV}^{1/2} , \\ \Gamma_0(\eta_b \rightarrow 2g) &= \left[\frac{\alpha_s}{0.13} \right]^2 3.18 \text{ MeV} , \\ \Gamma(\eta_b \rightarrow 2g) &= \left[\frac{\alpha_s}{0.13} \right]^2 4.58 \text{ MeV} , \quad (4.16) \\ \Gamma_0(\eta_b \rightarrow 2\gamma) &= 0.56 \text{ keV} , \\ \Gamma(\eta_b \rightarrow 2\gamma) &= 0.48 \text{ keV} ; \\ C_{\eta'_b} &= 0.043 \text{ GeV}^{1/2} , \\ \Gamma_0(\eta'_b \rightarrow 2g) &= \left[\frac{\alpha_s}{0.13} \right]^2 1.04 \text{ MeV} , \\ \Gamma(\eta'_b \rightarrow 2g) &= \left[\frac{\alpha_s}{0.13} \right]^2 1.50 \text{ MeV} , \quad (4.17) \\ \Gamma_0(\eta'_b \rightarrow 2\gamma) &= 0.18 \text{ keV} , \\ \Gamma(\eta'_b \rightarrow 2\gamma) &= 0.15 \text{ keV} . \end{aligned}$$

For the other cases the predicted values are listed in Table I.

C. The decay rates of η_c , η'_c , η_b , and η'_b to $2g$ and 2γ calculated by the Schrödinger equation or with relativistic Coulomb interactions

For comparison, the decay rates of η_c , η'_c , η_b , and $\eta'_b \rightarrow 2g$ and 2γ are also calculated by using the Schrödinger equation with a potential which is the same as the nonrelativistic limit of the interaction used in the relativistic calculation, i.e., the Richardson potential:¹⁵

TABLE I. Decay rates of η_c , η'_c , η_b , $\eta'_b \rightarrow 2g$ and 2γ and η_l , η'_l , η_s , $\eta'_s \rightarrow 2\gamma$ with QCD corrections for η_c , η'_c , η_b , η'_b . The quark masses are $m_c = 1.57$, $m_b = 4.9$, $m_l = 0.35$, $m_s = 0.55$ GeV. The QCD potential scale $\Lambda_R = 0.40$ GeV. The parameters for the QCD interaction are $\kappa_s = 0.15$, $\alpha_s(\eta_c) = \alpha_s(\eta'_c) = 0.15$, $\alpha_s(\eta_b) = \alpha_s(\eta'_b) = 0.13$. The parameters of the Coulomb interaction are $\kappa_s = 0.18$, $\alpha_{\text{eff}} = 0.52$.

	QCD $\epsilon = 0.25$	QCD $\epsilon = 1.0$	Coulomb $\epsilon = 1.0$	Schrödinger	Experimental
With QCD correction					
$\eta'_b \rightarrow 2g$ (MeV)	1.6	1.5	1.6	2.4	
$\rightarrow 2\gamma$ (keV)	0.17	0.16	0.17	0.25	
$\eta_b \rightarrow 2g$ (MeV)	5.0	4.6	6.2	5.6	
$\rightarrow 2\gamma$ (keV)	0.52	0.48	0.65	0.59	
$\eta'_c \rightarrow 2g$ (MeV)	3.1	2.7	3.0	4.2	< 8
$\rightarrow 2\gamma$ (keV)	3.6	3.2	3.4	4.9	
$\eta_c \rightarrow 2g$ (MeV)	13.1	11.5	11.8	9.5	11.5 ± 4.3
$\rightarrow 2\gamma$ (keV)	14.8	13.1	13.2	11.1	9.2 ± 3.8
Without QCD correction					
$\eta'_s \rightarrow 2\gamma$ (keV)	0.11	0.10	0.16	0.36	
$\eta_s \rightarrow 2\gamma$ (keV)	2.96	2.37	1.84	1.45	
$\eta'_l \rightarrow 2\gamma$ (keV)	0.62	0.62	1.10	3.2	
$\eta_l \rightarrow 2\gamma$ (keV)	25.4	20.7	15.5	16.6	

$$V_R(\mathbf{q}^2) = \frac{-4\pi \left[\frac{16\pi}{27} \right]}{\bar{q}^2 \ln(1 + \mathbf{q}^2 / \Lambda_R^2)}. \quad (4.18)$$

We use the same Λ_R parameter and compute without any cutoff.

In the comparison of the relativistic results with the Schrödinger results for the Richardson potential in Table I we find the following.

(a) For the $1S$ states the relativistic results start out smaller than the nonrelativistic in the b system, but, as the quark mass scale decreases, end up larger.

(b) For the $2S$ states the relativistic results are smaller than the Schrödinger results, dropping from 63% at the η'_b to 19% for the η'_s . This effect we find is due to the delocalization of the annihilation away from zero separation, which increases as the exchanged constituent quark gets lighter.

The above effect arises from the inclusion of the full relativistic propagators in Eq. (3.6) instead of replacing them by $-Mm$ or $-qm$ in the nonrelativistic (NR) limit. In Eq. (3.10) the logarithm term arises from angular integration over the relativistic propagators. The NR limit gives the integrand

$$\frac{p}{m} \frac{p}{2} (a-b) = \frac{p^2}{2m} g_0.$$

The momentum integral then gives $\psi(0)$. The relativistic form alters the larger $p \gtrsim m$ momentum region. For $2S$ waves where the momentum-space wave function has a node and changes sign, the decrease due to the logarithm in Eq. (3.10) leads to further cancellation and a decreased amplitude.

As a test of whether the asymptotic-freedom modification of the gluon exchange is relevant at these energies, we also calculate the decay rates using a relativistic Coulombic plus linear interaction, which is a relativistic generalization of the Cornell potential.⁵ The relativistic vector interaction is $4\pi\alpha_{\text{eff}}/q^2$ and the scalar part is the linear potential. We use the same parameters as those used in the Cornell calculations: namely, $\alpha_{\text{eff}}=0.52$, $\kappa_s=0.1826$. These results are listed in Table I under the column labeled Coulomb. The closeness of the results of the asymptotic freedom and Coulombic vector interactions show that these annihilation results, although occurring at short distance, are not evidence for the asymptotic-freedom form of the interactions.

V. TWO-PHOTON DECAYS OF η , η' , AND ι AND MIXING MODELS

Although we have treated η and η' relativistically in terms of their valence $q\bar{q}$ structure, we have not included many important features such as the annihilation multi-gluon intermediate states,¹⁶ more than three state mixing or dynamical multichannel mixing.¹⁷ We will, however, show the restrictions on mixing that our treatment with the simple model of η_1 , η_8 , and a glueball receive from the two- γ decay rates of the η and η' (Ref. 18) and the bound on the two- γ decay rate of the ι .¹⁹ In the simple

model, the η , η' , and ι state are considered as mixtures of⁶

$$\begin{aligned} |N\rangle &= \frac{1}{\sqrt{2}}(|u\bar{u}\rangle + |d\bar{d}\rangle), \quad |S\rangle = |s\bar{s}\rangle, \\ |G\rangle &= \text{gluon bound state}, \end{aligned} \quad (5.1)$$

with coefficients

$$\begin{aligned} |\eta\rangle &= X_\eta |N\rangle + Y_\eta |S\rangle + Z_\eta |G\rangle, \\ |\eta'\rangle &= X_{\eta'} |N\rangle + Y_{\eta'} |S\rangle + Z_{\eta'} |G\rangle, \\ |\iota\rangle &= X_\iota |N\rangle + Y_\iota |S\rangle + Z_\iota |G\rangle. \end{aligned} \quad (5.2)$$

For the two-photon decay, η , η' , or ι resulting from the charged $|N\rangle$ or $|S\rangle$ parts we have for Eq. (3.11) with the appropriate X and Y :

$$\langle Q^2 C \rangle = X \langle 0 | Q^2 C | N \rangle + Y \langle 0 | Q^2 C | S \rangle, \quad (5.3)$$

$$\langle Q^2 C \rangle = \frac{1}{\sqrt{2}} \left(\frac{4}{9} + \frac{1}{9} \right) X C_N + \frac{1}{9} Y C_S,$$

where the C_N and C_S in Eq. (3.10) arise from solutions to separate bound-state equations for the unmixed $|N\rangle$ and $|S\rangle$ states. The values we find are

$$C_N = 0.129 \text{ GeV}^{1/2}, \quad C_S = 0.155 \text{ GeV}^{1/2}, \quad (5.4)$$

with corresponding masses

$$M_N = 0.76 \text{ GeV}, \quad M_S = 0.96 \text{ GeV}.$$

It is important to note the relativistic result that the normalization conditions for the $|N\rangle$ and $|S\rangle$ states involves the eigenvalue masses M_N and M_S in Eq. (2.14) in a/\sqrt{M} , b/\sqrt{M} , and these masses must be used for each basis state separately in forming C_N and C_S in Eq. (3.10). This is different from the nonrelativistic form⁸

$$\Gamma_{\text{NR}} = 48\pi\alpha^2 \langle Q^2 \rangle^2 \frac{\psi(0)^2}{m_\eta^2}, \quad (5.5)$$

where the mixed-state mass occurs. The component rates for $\eta_l \equiv |N\rangle$ and $\eta_s \equiv |S\rangle$ decays separately are listed in Table I.

We include in the decay rate in Eq. (3.11) a higher-order QCD-correction factor r which we consider unknown at these low energies but assume it is the same for all of these decays in order to complete the analysis.

This gives

$$\Gamma(\eta \rightarrow 2\gamma) = r 48\pi\alpha^2 \left[\frac{1}{\sqrt{2}} \frac{5}{9} C_N \right]^2 \left[X_\eta + \frac{\sqrt{2}}{5} \frac{C_S}{C_N} Y_\eta \right]^2 \quad (5.6)$$

with similar equations for η' and ι decay, where

$$\sqrt{2} C_S / (5 C_N) \equiv q = 0.34. \quad (5.7)$$

Using the experimental rates^{18,19} on η and η' and the bound on ι ,

$$\begin{aligned} \Gamma(\eta \rightarrow 2\gamma) &= 0.56 \text{ keV} , \\ \Gamma(\eta' \rightarrow 2\gamma) &= 4.4 \text{ keV} , \\ \Gamma(\iota \rightarrow 2\gamma) &< 2.2 \text{ keV} , \end{aligned} \tag{5.8}$$

we have the conditions from Eq. (5.6)

$$X_\eta + qY_\eta = 0.165/r^{1/2} \equiv C_1 , \tag{5.9a}$$

$$X_{\eta'} + qY_{\eta'} = 0.46/r^{1/2} \equiv C_2 , \tag{5.9b}$$

$$X_\iota + qY_\iota \equiv C_3 < 0.33/r^{1/2} . \tag{5.9c}$$

By squaring and summing the equations in (5.9) and using the orthonormality conditions

$$\begin{aligned} X_\eta^2 + X_{\eta'}^2 + X_\iota^2 &= 1 , \\ Y_\eta^2 + Y_{\eta'}^2 + Y_\iota^2 &= 1 , \\ X_\eta Y_\eta + X_{\eta'} Y_{\eta'} + X_\iota Y_\iota &= 0 , \end{aligned} \tag{5.10}$$

we get

$$\begin{aligned} 1 + q^2 &= C_1^2 + C_2^2 + C_3^2 \\ &= \frac{(0.165)^2}{r} + \frac{(0.46)^2}{r} + C_3^2 . \end{aligned} \tag{5.11}$$

This equation relates r to C_3 .

Using $0 \leq C_3^2 \leq (0.33)^2/r$ of Eq. (5.9) in Eq. (5.11)

gives the bounds

$$0.21 \leq r \leq 0.31 . \tag{5.12}$$

For the range of values of C_3 or $\Gamma(\iota \rightarrow \gamma\gamma)$ which is allowed by the bound, Eq. (5.8), we now find the restrictions on the mixing parameters. There are six independent variables, X 's and Y 's, and five independent conditions, Eqs. (5.9) and (5.10) related by Eq. (5.11). For each choice of C_3 or $\Gamma(\iota \rightarrow \gamma\gamma)$ we have a range of solutions as a function of one independent variable, say X_η .

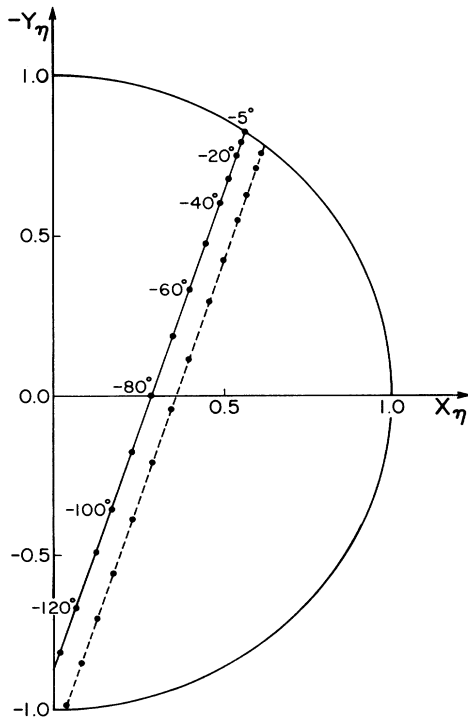


FIG. 2. Solutions for mixing parameters $-Y_\eta$ as a function of X_η for the cases $\Gamma(\iota \rightarrow 2\gamma) = 2.2 \text{ keV}$ (solid line) and $\Gamma(\iota \rightarrow 2\gamma) = 0$ (dashed line). The corresponding θ_1 mixing angle is also shown.

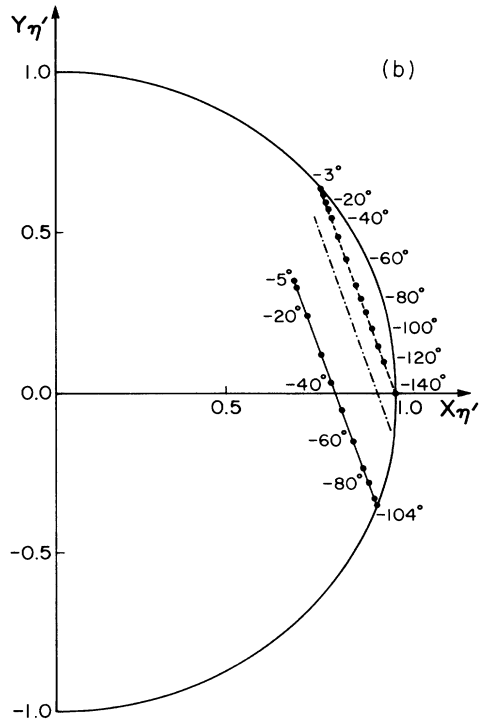
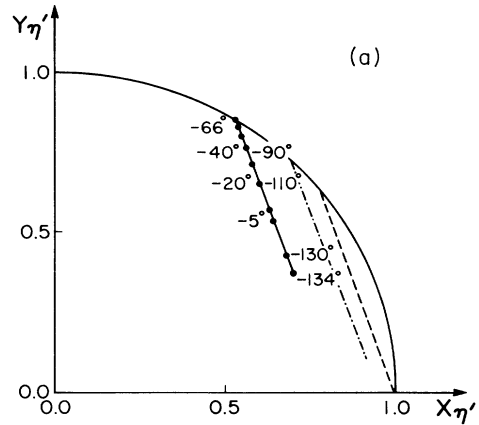


FIG. 3. Solutions for mixing parameters $Y_{\eta'}$ and $X_{\eta'}$ for the cases $\Gamma(\iota \rightarrow 2\gamma) = 2.2 \text{ keV}$, 1.1 keV , and 0 as solid line, dot-dashed, and dashed lines, respectively. (a) corresponds to the (+) branch in Eq. (5.13) and (b) to the (-) branch.

Solving the set of equations for $X_{\eta'}$ as a function of X_{η} , gives

$$X_{\eta'}^{\pm} = \frac{1}{C_2^2 + C_3^2} \left\{ -C_2(X_{\eta}C_1 - 1) \pm C_3[q^2(1 - X_{\eta}^2) - (X_{\eta} - C_1)^2]^{1/2} \right\}. \quad (5.13)$$

The boundaries on X_{η} occur when the square root in Eq. (5.13) vanishes:

$$X_{\eta}^{\pm} = \frac{C_1 \pm q(1 + q^2 - C_1^2)^{1/2}}{1 + q^2}. \quad (5.14)$$

The curves for $X_{\eta'}$ versus Y_{η} arise directly from Eq. (5.9a) with r depending on the assumed value of C_3 . These are shown in Fig. 2. The curves for $X_{\eta'}$ versus Y_{η} from Eq. (5.9b) are shown in Figs. 3(a) and 3(b). Points in Fig. 3 are connected to those in Fig. 2 by Eq. (5.13) as shown in Fig. 4. For $\Gamma(\iota \rightarrow 2\gamma) = 2.2$ keV, 1.1 keV, or 0, the r values are 0.31, 0.24, and 0.21, respectively.

The standard mixing angle analogous to the Cabibbo angle for the mixing of η_8 , η_1 , and G to η , η' , ι in a 3×3 Kobayashi-Maskawa (KM) matrix analog can be obtained from

$$\cos\theta_1 = \langle \eta | \eta_8 \rangle = \frac{1}{\sqrt{3}} \langle \eta | N \rangle - \left(\frac{2}{3}\right)^{1/2} \langle \eta | S \rangle, \quad (5.15)$$

$$\theta_1 = -\arccos \left[\frac{1}{\sqrt{3}} X_{\eta} - \left(\frac{2}{3}\right)^{1/2} Y_{\eta} \right],$$

where the minus sign arises because of opposite signs in the definition of the mixing angle from the Cabibbo angle.

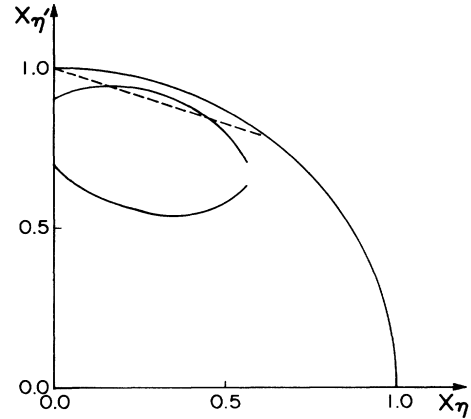


FIG. 4. Connection of values of $X_{\eta'}$ to those of X_{η} as given by Eq. (5.13). The dashed curve is for $\Gamma(\iota \rightarrow 2\gamma) = 0$. The upper and lower solid curves are for the (+) and (-) branches of Eq. (5.13) with $\Gamma(\iota \rightarrow 2\gamma) = 2.2$ keV.

We see from Figs. 2 and 3(a) that for small $\Gamma(\iota \rightarrow 2\gamma)$ there are solutions near the circles where there is little glueball mixing into η and η' and with mixing angles in the range -5° to -20° .

ACKNOWLEDGMENTS

We wish to thank M. Bander, F. Daghighian, S. Meshkov, and S. Pinsky for discussions, and the Aspen Center of Physics for its hospitality. This work was supported in part by the National Science Foundation under Grant No. PHY 8605552.

¹M. Bander, D. Silverman, B. Klima, and U. Maor, Phys. Rev. D **29**, 2038 (1984).

²M. Bander, D. Silverman, B. Klima, and U. Maor, Phys. Lett. **134B**, 258 (1984).

³O. Greenberg, Phys. Rev. **139B**, 1038 (1965); O. Greenberg and R. Genolio, Phys. Rev. **150**, 1070 (1966); F. Gross *ibid.* **186**, 1448 (1969); K. Johnson, Phys. Rev. D **4**, 1101 (1972).

⁴G. P. Lepage, Phys. Rev. A **16**, 863 (1977); W. Caswell and G. P. Lepage, *ibid.*, **20**, 36 (1979).

⁵E. Eichten, K. Gottfried, T. Kinoshita, K. Lane, and T. Yan, Phys. Rev. Lett. **36**, 500 (1976); Phys. Rev. D **17**, 3090 (1978); **21**, 313 (1980); **21**, 203 (1980).

⁶J. Rosner, Phys. Rev. D **27**, 1101 (1983); S. Meshkov, in *Proceedings of the Aspen Winter Physics Conference, 1986*, edited by Loyal Durand [Ann. N.Y. Acad. Sci. **490**, (1987)].

⁷J. Bjorken and S. Drell, *Relativistic Quantum Fields* (McGraw-Hill, New York, 1965), Chap. 16.

⁸F. Close, *An Introduction to Quarks and Partons* (Academic,

New York, 1978), Chap. 16.

⁹Particle Data Group, Phys. Lett. **170B**, 215 (1986); Crystal Ball Collaboration, J. Gaiser, *et al.*, Phys. Rev. D **34**, 711 (1986).

¹⁰R. Barbieri, R. Gatto, R. Kögerler, and Z. Kunszt, Phys. Lett. **57B**, 455 (1975); R. Barbieri, G. Curci, and E. d'Emilio, Nucl. Phys. **B154**, 535 (1979); R. Barbieri, R. Caffo, M. Gatto, and R. Remiddi, Phys. Lett. **95B**, 93 (1980); Nucl. Phys. **B192**, 61 (1981); R. Barbieri, R. Gatto, and E. Remiddi, Phys. Lett. **106B**, 497 (1981); S. Brodsky, G. P. Lepage, and P. Mackenzie, Phys. Rev. D **28**, 228 (1983); W. Kwong, J. Rosner, and C. Quigg, Annu. Rev. Nucl. Part. Sci. **37**, 1987.

¹¹W. Caswell, Phys. Rev. Lett. **33**, 244 (1974); D. Johnes, Nucl. Phys. **B75**, 531 (1974); P. Mackenzie and G. P. Lepage, Phys. Rev. Lett. **47**, 1244 (1981).

¹²S. Cooper, in *Proceedings of the XXIII International Conference on High Energy Physics*, Berkeley, California, 1986,

- edited by S. Loken (World Scientific, Singapore, 1987); Report No. SLAC-Pub-4139, 1986, (unpublished).
- ¹³C. Baylin *et al.* Phys. Lett. B **171**, 135 (1986).
- ¹⁴R. Barbieri *et al.* Phys. Lett. **106B**, 497 (1981).
- ¹⁵J. Richardson, Phys. Lett. **82B**, 272 (1979); R. Carlitz and D. Creamer, Ann Phys. (N.Y.) **118**, 429 (1979); R. Levine and Y. Tomozawa, Phys. Rev. D **21**, 840 (1979).
- ¹⁶S. Godfrey and N. Isgur, Phys. Rev. D **32**, 189 (1985).
- ¹⁷W. F. Palmer, S. S. Pinsky, and C. Bender, Phys. Rev. D **30**, 1002 (1984); S.-C. Chao, W. F. Palmer, and S. Pinsky, Phys. Lett. B **172**, 253 (1986).
- ¹⁸A. Weinstein, Phys. Rev. D **28**, 2896 (1983); W. Bartel *et al.* Phys. Lett. **158B**, 511 (1985); Particle Data Group, Phys. Lett. **170B**, 117 (1986); **170B**, 182 (1986).
- ¹⁹H. Aihara *et al.* Phys. Rev. Lett. **57**, 51 (1986).